

Atomic Scale Chemical Mapping in SrO(SrTiO₃)₆ Ruddlesden-Popper Thin Film

Ye Zhu,* Che-Hui Lee,***** Darrell G. Schlom,** David A. Muller*

* Department of Applied and Engineering Physics, Cornell University, Ithaca, NY 14853

** Department of Materials Science and Engineering, Cornell University, Ithaca, NY 14853

*** Department of Materials Science and Engineering, Penn State University, University Park, PA 16802

Introducing rock-salt layers (AO) into the perovskite structure (ABO₃), divides the perovskite structure into thin quasi-two-dimensional oxide sheets separated by anti-phase boundaries comprised purely of AO-bonded materials. When periodically ordered, this gives rise to Ruddlesden-Popper materials (AO(ABO₃)_n) which can be designed for a variety of properties such as high-T_c superconductivity [1] or low-loss dielectrics [2], depending on the choice of A and B-site cations. Using molecular beam epitaxy (MBE) deposition, SrO(SrTiO₃)_n ($n = 1-6, 10$) thin films were synthesized on (110) DyScO₃ substrates, and among them the SrO(SrTiO₃)₆ film showed the highest figure of merit ($FOM = \Delta\epsilon/\epsilon/\tan\delta$) of all known tunable dielectrics, including SrTiO₃ and (Ba,Sr)TiO₃ (Fig. 1a) [3]. Such a high FOM is attributed to the low point defect density inside the SrO(SrTiO₃)₆ film.

In this work, we used aberration-corrected electron microscopy to investigate the structure and chemistry of the SrO(SrTiO₃)₆ sample. Despite its thermodynamic instability as a bulk phase [4], the SrO(SrTiO₃)₆ phase was successfully synthesized by MBE as verified by the high-resolution Z-contrast image in Fig. 1b. However, besides the horizontal SrO layers as in the SrO(SrTiO₃)₆ unit cell, vertical SrO faults were also present so that the (SrTiO₃)₆ slabs were divided into nano-bricks to form the 'brick-wall' structure (Fig. 2c). From the image like Fig. 2c, the average spacing between vertical SrO faults was estimated to be ~7 nm. With such a high density of SrO layers along both directions the film still exhibit the highest FOM, which makes it interesting to explore the electronic structure of SrO layers and its effects on dielectric properties.

Figure 2 shows EELS maps taken across a horizontal SrO layer. In both Ti and O maps (Fig. 2(b) and (c)) we can see a half unit cell shift across the SrO layer. Besides the lower O density around the SrO layer, the O K-edges also show different fine structure as seen in Fig. 2(f). The first peak of the O spectrum is considerably lower around the SrO layer, consistent with the fact that this peak is related to the hybridization of the O 2p and Ti 3d orbitals. Fitting the two spectra in Fig. 2(f) to the O data gives the concentration of the two components, as shown in the 1D profile in Fig. 2(d). The low-pre-edge O component is clearly localized around the SrO layers. On the other hand, Ti edges taken from the SrTiO₃ lattice and around the SrO layer show little difference, indicating no Ti valence change. For the next step, EELS simulation based on density functional theory will be performed to further interpret the O spectrum from SrO layers. Quantitative comparison between experimental and simulated spectra might provide better understanding of the chemistry and electronic structure in SrO layers. [5]

[1] H. Müller-Buschbaum, *Angew. Chem., Int. Ed. Engl.* **28**, 1472 (1989).

[2] P. L. Wise, I. M. Reaney, W. E. Lee, T. J. Price, D. M. Iddles, and D. S. Cannell, *J. Eur. Ceram. Soc.* **21**, 2629 (2001).

[3] N. D. Orloff, "Broadband In-plane Relative Permittivity Characterization of Ruddlesden-Popper $\text{Sr}_{n+1}\text{Ti}_n\text{O}_{3n+1}$ Thin Films," Ph.D. Thesis (University of Maryland, 2010). Available on-line at <http://drum.lib.umd.edu/handle/1903/11063>.

[4] C. Noguera, *Philos. Mag. Lett.* **80**, 173 (2000).

[5] Work supported by ARO #W911NF0910415, and facilities NSF DMR# 0520404

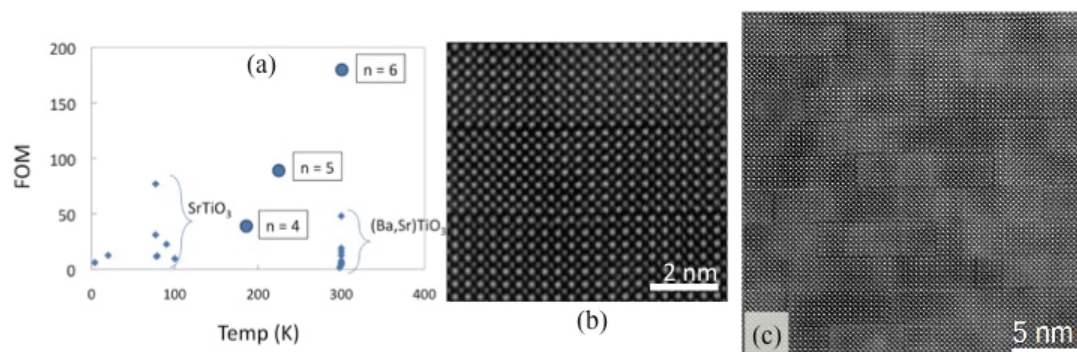


FIG. 1. (a) Figure of merit ($\Delta\epsilon/\epsilon/\tan\delta$ in GHz) vs. temperature plot for various materials. (from ref. 3) (b) HAADF image showing the perfect $\text{SrO}(\text{SrTiO}_3)_6$ lattice. (c) HAADF image showing the brick-wall structure of the $\text{SrO}(\text{SrTiO}_3)_6$ film.

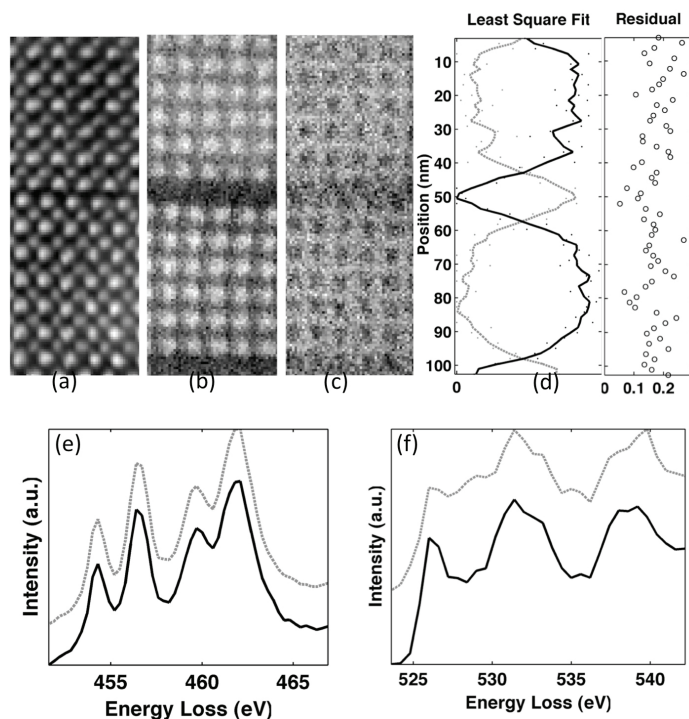


FIG. 2. (a) HAADF image, (b) Ti EELS map, (c) O EELS map taken from the $\text{SrO}(\text{SrTiO}_3)_6$ lattice. A rock-salt SrO layer is at the middle. (d) O 1D profile showing distribution of the two O components (see (f)). The residual to the fit is on the right. (e) Ti L-edges and (f) O K-edges taken from the SrTiO_3 lattice (black solid line) and around the rock-salt SrO layer (grey dashed line), respectively. O K-edges show different 1st peak heights, while Ti edges are essentially the same.